Dissolution kinetic study of limonene in supercritical carbon dioxide by *in-situ* Raman spectroscopy

Cristiana Nilsson Buzolin

Master Thesis in Analytical Chemistry, 2016
Department of Chemistry
Lund University
Sweden

Dissolution kinetic study of limonene in supercritical carbon dioxide by *in-situ* Raman spectroscopy

Cristiana Nilsson Buzolin

Master Thesis in Analytical Chemistry

2016

Advisor:

Irene Rodríguez-Meizoso

Lund University

Examiner:

Charlotta Turner

Lund University

Centre for Analysis and Synthesis

Department of Chemistry

Lund University, Box 124

SE-221 00 Lund, Sweden

Popular Science: Is carbon dioxide an enemy of the planet but a friend of science?

Carbon dioxide (CO_2) is a colourless and odourless gas present in all living organisms and the entire atmosphere on Earth. The molecule is formed by one carbon and two oxygen atoms**.** It is an essential molecule for plants to make the photosynthesis process, which produces the oxygen we breathe. It is also the main product of plant and animal respiration and burning process such as forest fires and volcanic eruptions.[1] Levels of carbon dioxide would be well-regulated in the atmosphere if human interference did not exist. Nowadays, increasing levels of the gas as a result of mankind's activities are intensifying the greenhouse effect, a natural phenomenon essential for making Earth's atmosphere warm enough to support life, and therefore making carbon dioxide to be seen as a global issue.

In the chemistry field, on the other hand, carbon dioxide is not seen as a threat but a solution. At a certain pressure and temperature (74 bar and 31ºC), that is above our surrounding conditions but still quite mild for chemical applications, CO_2 can reach a state called supercritical and become a fluid. Beyond these values, CO_2 present improved properties than as a gas, allowing it to work as a solvent. This means that some substances can be dissolved in it to a certain extent. Compared to toxic organic solvents commonly used in chemistry, such as hexane, CO_2 is non-toxic, non-flammable, cheaper, abundant, renewable and therefore a better option. [2,3] Examples of industrial applications with CO_2 as a supercritical fluid involve extraction processes, such as removal of caffeine from coffee (decaffeination), particle size control of active pharmaceuticals ingredients (in order to improve its deliver in the human body), surfaces cleaning and textile dyeing. [2-6]

In the scientific area, very little is known about how fast substances are completely dissolved in supercritical CO_2 ($scCO_2$) with time, which are called kinetic studies. Pressure and temperature changes can also affect the dissolution speed. Understand such a system can help chemical processes by determining the best conditions to save time, control amount of substance used and improve yield, all relevant for an industry, since money is involved.

One such study concerns the use of high pressure and temperature. The mixture of substance+$scCO_2$ is commonly placed inside a sealed vessel to keep the conditions. Now imagine how hard it would be if a small amount of this mixture had to be taken out of the vessel to be analyzed without affecting the pressure and temperature. To overcome this problem, there is technique called *in situ*, that is analyzing the mixture directly inside the vessel. In the present work, *in-situ* Raman spectroscopy technique will be used. Spectroscopy is any study that involves the interaction of a matter with light. In the case of Raman, the light source is a laser, like the ones used as pointers, but at a much higher power. Basically, a powerful laser will be pointed to the mixture and through interactions undetectable by the naked eye, the energy of the laser will be split into lower energies, same is to say that the light will be scattered. This scattering is very specific for each substance and it is seen in form of peaks in a spectrum, which can be called the ID or fingerprint of your substance in the Raman.

In this work dissolution kinetics of limonene in $scCO_2$ was studied at different combinations of pressure and temperature inside a vessel by *in-situ* Raman spectroscopy. The curve fitting of the processed data showed that the solubility kinetics can be described by a first order exponential equation. Dissolution rate values of the fitted curves showed that the kinetic of solubility is faster at lower pressures and temperatures.

Abstract

Understanding the dissolution kinetics is important in the experimental determination of solubility, the efficiency of extractions, the rate of reactions and in general any heterogeneous process. Despite the extensive use of supercritical fluids, studies regarding the dissolution kinetics of compounds in supercritical carbon dioxide ($scCO_2$) using analytical methods are limited in the literature. So far, only one work can be found where acetaminophen was used as model compound and *in-situ* Infrared spectroscopy was used to investigate the dissolution kinetics for two different temperatures at the same pressure. A more common approach involving $scCO_2$ as a solvent is the study of the kinetic of reactions, such as catalyzed organic reactions and polymerizations by the common *in-situ* spectroscopy techniques (IR, UV-Vis and Raman).

In this work, the dissolution kinetic behaviour of limonene in $scCO_2$ was studied at different combinations of pressure and temperature by *in-situ* Raman spectroscopy. The experiments were carried out inside a high-pressure constant-volume view cell. The instrumental setup consisted of a pressurized system and a linear Raman optical system, where a continuous-wave laser at 3.5 W and a wavelength of 532 nm were used. A peak correspondent to a C=C stretching mode from limonene (583-584 nm) was monitored with time, where the height is directly proportional to the amount solubilized in carbon dioxide (CO_2).

The experiments were carried out at temperature of 45 ºC and 55 ºC and pressure ranging from 84 to 163 bar. The time of the experiments ranged between 100 and 420 minutes. The time to reach complete dissolution varies significantly with pressure and temperature (from 30 min up to 4 hours). Curve fitting of the processed data showed that the solubility kinetics can be described by a first order exponential model. Dissolution rate values of the fitted curves showed that the rate of dissolution becomes slower with increase of pressure and temperature, in contradiction to conventional dissolution theory for liquid solvents. Experiments to evaluate the stirrer effect on the dissolution showed that for the lowest pressures tested at 45 °C and 55 °C (respectively 84 and 95 bar) stirring accelerates the process significantly, while for higher pressures stirring does not make a difference. These results are an indication that different mechanisms may govern dissolution kinetics, depending on the region of pressure and temperature studied. Thus, the results constitute the first step towards a theoretical understanding of the mechanisms of dissolution kinetics of solutes in supercritical fluids.

Keywords: Raman spectroscopy, supercritical carbon dioxide, limonene, dissolution kinetics, solubility

Acknowledgement

I want to thank you Irene Rodríguez-Meizoso for the wonderful supervision, great ideas and advices, both professional and personal.

Thank you to all members of the CAS group for all the support and pleasant work environment.

Thank you to all my friends in Lund, who makes my days great outside the university.

Thank you to my family that, despite the distance, always supported me with my studies.

Abbreviations

ALS	Asymmetric Least Squares
CCD	Charge coupled device
CO_2	Carbon dioxide
H	Peak height
IR	Infrared
K	Dissolution rate
LOD	Limit of detection
P	Pressure
$scCO_2$	Supercritical carbon dioxide
SCF	Supercritical fluid
SD	Standard deviation
T	Temperature
t	Time
UV	Ultraviolet
ρ	Density

Table of Contents

1 Introduction

A supercritical fluid (SCF) is any substance above its critical pressure and temperature, known as the critical point (Figure 1). At this point, high diffusivity and low viscosity rates are reached, with values between those observed for gas and liquid states. [2,3] Small changes in pressure and temperature can cause large changes in density, allowing the fluid solvent power to be fine-tuned.

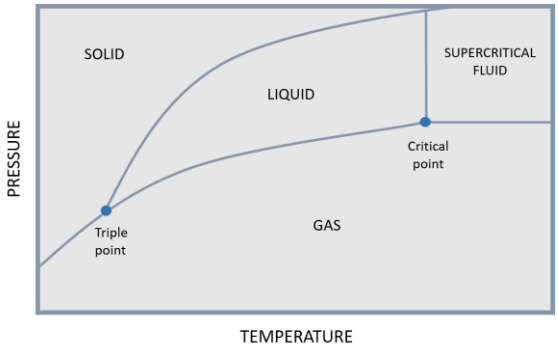

Figure 1. Phase diagram of pressure *vs.* temperature.

Carbon dioxide is one of the most used SCF, mainly because it presents a mild critical point, close to ambient conditions (31.1ºC, 73.8 bar). [2] Moreover, it is nonflammable, non-toxic for humans, naturally occurring and an industrial byproduct in many large scale processes. [2,3] All these attributes can classify supercritical carbon dioxide ($scCO_2$) as a green solvent and an alternative to conventional organic solvents. Besides, because it is a non-polar solvent, a polar cosolvent can be usually added in small quantities to enhance the solubility power for polar compounds.

Solubility experimental data of many compounds in $scCO_2$ can be found in the literature [2,7,8], but due to the different techniques used to determine it, the values can vary a lot for a same compound. For high-pressure phase equilibria studies, the classification found in the literature can be very controversial according to different authors. The methods can be divided in two major categories: static and dynamic. [2,7,8] In static methods, the solute is placed in contact with the $scCO_2$ until the system reaches equilibrium while in dynamic methods the fluid is continuously pumped through the vessel containing the solute and the saturated solution flowing out is analyzed. [2] However, sometimes both methods are classified as "dynamic" and a less ambiguous categorization divides the methods in analytical and synthetic, branched from the static methods. [2,7,8] The difference between them is regarding the analysis of the phases composition. In the analytical method, the phases can be analyzed after sampling or analyzed directly without sampling by spectroscopic techniques. [2,7,8] For the synthetic methods, the amounts of solute and solvent are precisely known and the overall composition of the system is analyzed without sampling, towards the appearance/disappearance of phases by changing pressure or temperature independently. [2,7,8]

In the analytical methods, sampling techniques that provide information about the dependent relation between analyte concentration and its dissolution extent in the solvent are limited to precision sampling and *in situ* analysis. The first is based on taking samples at different increments of time and subsequent analysis. The challenge of such technique is to take a sample of a sealed system under high pressure with precision and without disturbing the equilibrium (pressure drop).[8]

Because of that, the *in situ* technique, where the analysis is done directly inside the equilibrium view cell, is an advantage.

In situ techniques for online monitoring chemical concentrations or reaction kinetics mainly involves spectroscopic methods such as Ultraviolet (UV), Infrared (IR) and Raman spectroscopy. The main advantage of *in situ* analysis is that no sample preparation is required. For UV spectroscopy, it is only possible to monitor molecules carrying chromophores. For IR and Raman spectroscopy, extra care must be taken regarding the possible light absorption and fluorescence given by the window cells.

Raman spectroscopy is regarded as an analytical technique where the molecule interacts with the incident monochromatic radiation provided by a laser. The result is a weak inelastic scattered light caused by the vibrational modes of the molecule shifting the laser frequency.[9] Figure 2 illustrates a simplified scheme of the Raman phenomenon. Only vibrational modes that are able to change the molecule polarizability, i.e. change in the charge distribution, are active in Raman.[9] The light is scattered by the analyte at different wavelengths, which correspond to different peaks in the spectrum. Thus, this technique is able to detect all organic compounds and due to the high spectrum resolution, resulting in sharp peaks, mixture of compounds can also be studied. Beyond that, it is a complementary technique to IR spectroscopy, since some Raman-active modes are IR-inactive.[9]

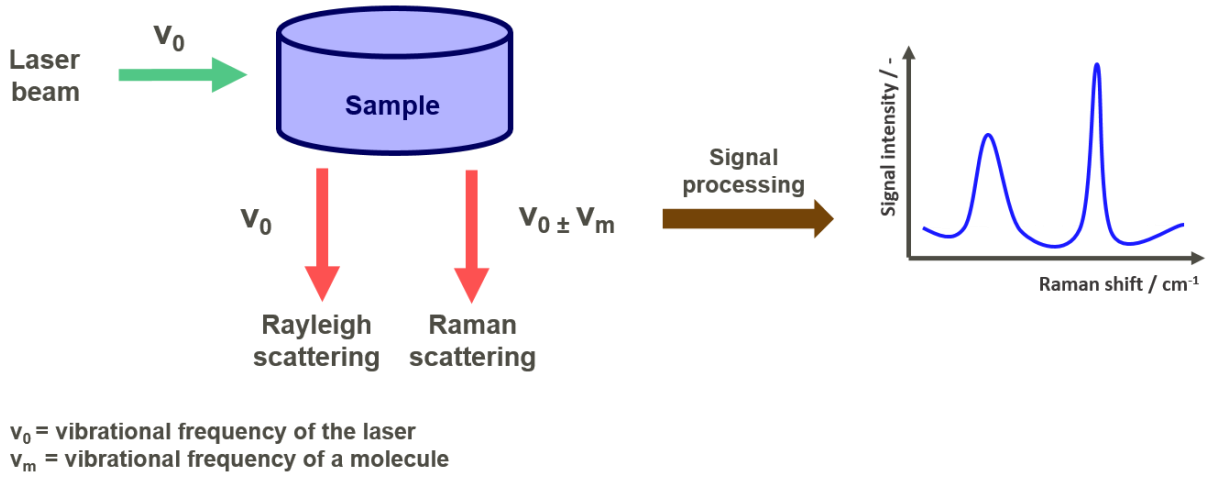

Figure 2. Simplified Raman spectroscopy scheme.

Raman spectroscopy is considered a low-probability process, where only one out of 10^8 photons is likely to be inelastic scattered.[10] Another limitation is that Raman can be affected by fluorescence, which is the emission of light by a molecule after excited with an electromagnetic radiation (Figure 3).[11] The light emitted has a larger wavelength, i.e. lower energy than the absorbed light. This phenomenon affects the spectrum, resulting in high baselines and hindering the compounds peaks to be clearly seen. The compound itself can fluoresce and for this case, a baseline correction is recommended.

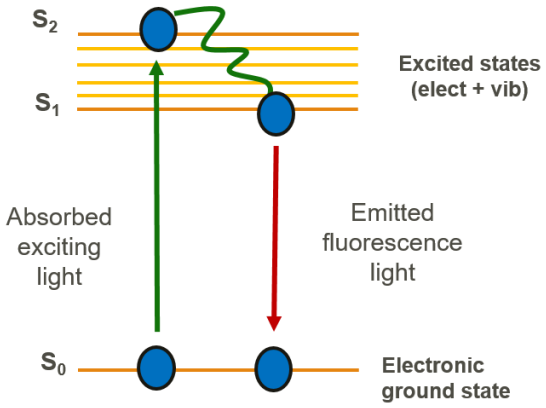

Figure 3. Fluorescence scheme for a molecule.

The usual detector used is the charge coupled device (CCD), due to its high sensitivity to light. The detector basically stores the charge (electrons) generated by the scattered light in pixels evenly distributed in a two dimensional silicon-based array. The stored charge is proportional to the intensity of the photons striking the plate. The readout is done row by row, one pixel at a time.[12] The detector is non-destructive, provide a good resolution of peaks and records the spectrum at all wavelengths at once.

Another important feature regarding CCD is that the limit of detection (LOD) for any analyte can be improved by changing the detector parameters, such as the grating, the binning and the acquisition time. Grating determines the range of wavelengths that will pass through the exit slit before the detector. That is because light at different wavelengths is diffracted in different angles by the grating, orienting only certain wavelengths to reach the detector (Figure 4). A higher grating improves resolution, although narrows the spectral region.[12] The binning speeds up the readout pattern of the pixels in the CCD by accumulating electrons. The signal to noise ratio is improved, although reduces spatial resolution.[13] The initial intensity of the vibrational modes (i.e. the peaks) detected accounts for the analyte.

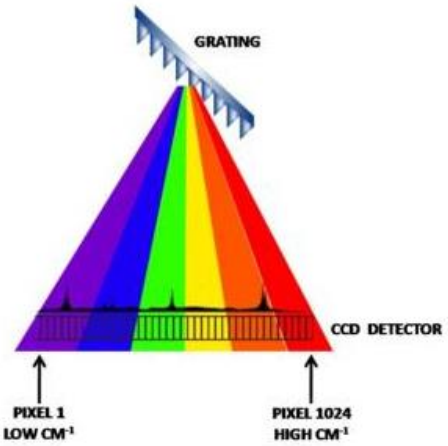

Figure 4. Scheme of light diffracted by the grating before reaching the detector. [14]

Among the several applications of supercritical CO_2 extraction of solids and liquids from natural materials, particle formation, polymer processing, surface cleaning and textile dyeing can be pointed out. [2-6] In the best case scenario, solubility data for a particular system has been used to develop these processes. However, very little is known about the kinetics of dissolution process of compounds in $scCO_2$, as well as in general SCFs, since this mechanism can vary for different combinations of pressure and temperature. Understanding the dissolution kinetics of compounds in $scCO_2$ would help chemical processes by determining the operating conditions to achieve the optimum set of time, reagent consumption and yield.

Studies regarding the dissolution kinetics of compounds in $scCO_2$ using analytical methods are limited in the literature. So far, only one work can be found where acetaminophen was used as model compound and *in-situ* IR spectroscopy was used to investigate the kinetics. The authors studied only two temperatures at a constant pressure. The compound dissolution exhibited either one slow step or two steps, a fast and a slow one, depending on region of the supercritical regime.[15] More common in situ kinetic studies involve the study of reaction kinetics, such as catalyzed organic reactions and polymerizations by the common *in-situ* spectroscopy techniques.[16-24]

There is currently no theory that explains dissolution kinetics of small organic compounds in $scCO_2$. Once the kinetic mechanism of a compound is established, application of theoretical models which describe and predict the observed results would be a step further for a deeper investigation not yet addressed in the scientific area.

To begin the studies of dissolution kinetics in $scCO_2$, the model compound chosen to be studied was limonene. Limonene is classified as an enantiomeric cyclic terpene, mostly found in the *d*-isomer configuration (Figure 5). At ambient conditions is a colorless liquid with a citrus odor. As an essential oil, is mainly used in the food and perfumery industry as flavoring and fragrance, respectively.[25] It is also the main component of the orange oil, accounting for 90% of the composition, followed by linalool.[26,27] With a very high solubility in CO_2 even at lower pressures and temperatures [2], limonene can easily be separated from essential oils in supercritical extraction processes. The use of a mild temperature prevents the compound thermal degradation, what usually happens when steam distillation, the most common technique to extract essential oils, is applied.[25,28]

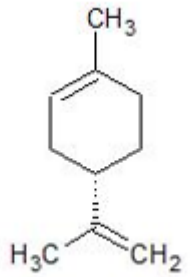

Figure 5. Molecular structure of *d*-limonene.

In the present work, dissolution kinetics of limonene will be studied in $scCO_2$ at different combinations of pressure and temperature inside a high-pressure view cell. The system will be analyzed by the *in-situ* Raman spectroscopy technique with a setup consisting of a pressurized and an optical system, where parameters for data acquisition can be optimized. It is worth mentioning that an entire new analytical methodology was developed to enable such investigation.

2 Aim and Research Questions

Develop an analytical methodology for the study of dissolution kinetics of model compounds in $scCO_2$ using a high-pressure view cell by *in-situ* Raman spectroscopy. It includes to determine the operational steps, optimize the data acquisition parameters, minimize the source of errors and find suitable software to process the data.

There are some challenges to overcome, such as improve the low Raman sensitivity due to the low intensity of the scattered light. This can be reached through the laser power and alignment and/or by changing the detector parameters (i.e. acquisition time, grating, binning, etc.). Another challenge is to develop operational steps in a specific order in a way that a problem in one of them can be corrected in time without affecting the previous ones, e.g. checking for gas leaking before increasing the pressure and temperature inside the view cell.

Through the proposed aims and challenges, the research questions are:

- ✓ How fast can a compound be dissolved in $scCO_2$?
- ✓ How much is the dissolution rate affected by pressure and temperature?
- ✓ Is the new developed analytical methodology quantitative?

3 Experimental

3.1 Materials

Limonene (CAS 5989-27-5, purity 97.0%) was supplied by Sigma Aldrich (USA). Carbon dioxide (CAS 124-38-9, purity 99.9993%) was supplied by AGA (Sweden).

3.2 Instrument setup

3.2.1 Equipment description

Figure 6 shows the scheme of the instrument setup, where a high-pressure constant-volume view cell is used. The setup consists of two parts: a pressurized system and an optical system.

Pressurized system: the view cell capacity is around 80 mL. The CO_2 was delivered in liquid state by a high-pressure syringe pump (Isco 100DX, Teledyne Technologies Inc., NE, USA). The lines are 1/16 in. stainless steel tubes and the flow is controlled by needle valves strategically situated. The pressure was measured by a pressure gauge. The view cell was heated by a heating tape and the temperature inside the vessel was measured by a thermocouple. A magnetic stirrer

was placed inside the vessel and moved by an external stirrer. A burst disc was placed for safety measure.

Optical system: the laser is a continuous wavelength of 532 nm with a maximum power of 5 W (Millennia Edge, Spectra Physics, Santa Clara, CA). The detector is a Shamrock 303i Spectrograph with a Newton 971 EMCCD Camera (Andor, Belfast, UK). All the lenses and mirrors are spherical, with 1" of diameter. The beam is expanded from 2 mm to 25.4 mm by a bi-concave lens and it is collimated by a plane-convex lens. The lenses used to focus the beam are achromatic, with focal length 100 mm and with antireflective coating. A dichroic beam splitter (DBS) for 532 nm, with a transmission above 94%, reflects the beam into the sample. A long pass filter with a transmission edge above 547 nm of more than 93% is placed between the DBS and the lens that focuses the Raman light into the detector. The chiller for the camera is a 300-watt Oasis Three. At the computer, the program used to acquire the data was Andor Solis, a software for imaging applications.

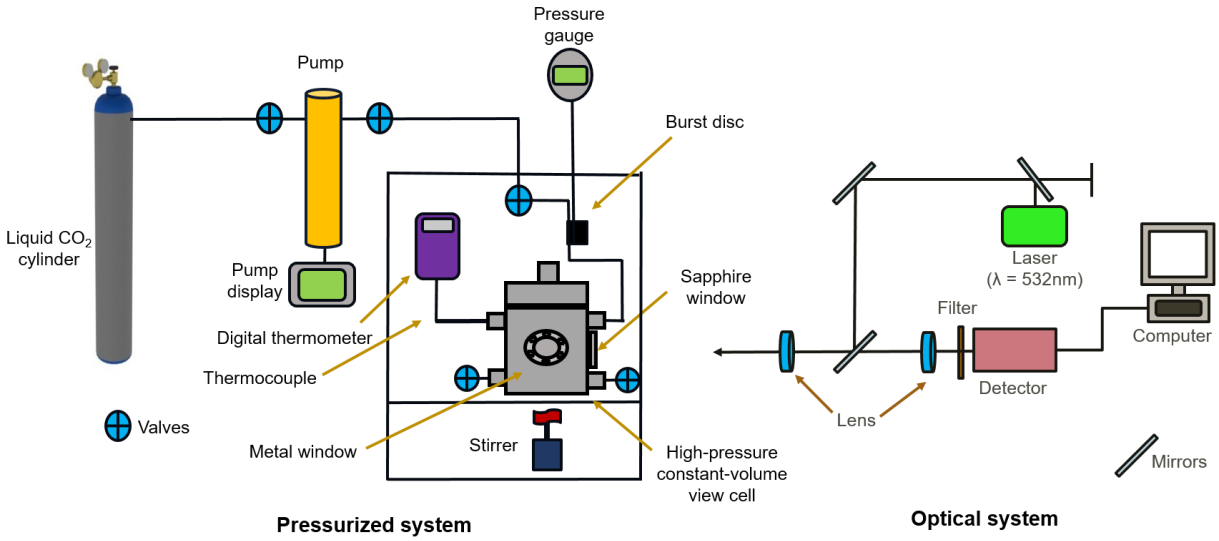

Figure 6. Instrumental setup consisting on a pressurized system with a high-pressure constant-volume view cell and an optical system.

3.2.2 Experimental procedure

Liquid CO_2 from the cylinder feeds the pump, where it is kept at a temperature of 5ºC. With the pump display, it is possible to set up the CO_2 pressure before the injection into the view cell. It also shows the amount of CO_2 injected in milliliters.

According to Figure 6, the upper right valve connected to the view cell injects the gas, while the lower left valve releases it. A heating tape (not shown) with an adjustable temperature is placed around the view cell. As the heat transfer from outside to inside is slow, the real temperature in the vessel interior is measured by a digital thermometer connected to a thermocouple placed inside through the upper left valve. Before filling up with the desired amount of CO_2, the view cell interior is purged with the gas and possible leakages through the valves are also checked. The gas injection is directly related to the increase of pressure and change in the solution composition. The

temperature is increased by the heating tape involving the view cell. Detailed steps are described in APPENDIX B.

Table 1 shows the order of operational steps. The laser alignment refers to center the sapphire window in the direction of the laser beam. This procedure is done with the laser on at power low enough to not cause any harm due to possible reflections. Then, the closest lens is placed at a specific distance where the laser focus falls inside the view cell. The time zero for the dissolution kinetics is considered at the moment the first spectrum is acquired. The stirrer is turned on after filling up the view cell with CO_2 and the first spectrum is acquired.

Table 1. Basic steps for the experiments.

1	View cell cleaning	**6**	Laser alignment
2	Addition of the sample	**7**	CO_2 injection (pressure increase)
3	Check for leakages	**8**	Stirrer on
4	Purge with CO_2	**9**	Spectrum acquisition
5	Temperature stabilization	**10**	Data processing

3.3 Dissolution kinetic experiments

The first step to study the dissolution kinetics is to acquire the Raman spectrum for the neat compound without CO_2 in order to identify and determine the peak signal that would be suitable to monitor during the experiment. Once chosen, the experiment in scCO_2 at different pressure and temperature at the optimized instrument parameters can be initiated.

Limonene was studied at four different pressures and two temperatures, as shown in Table 2. As described in section 3.2, the volume of CO_2 leads to a direct increase in the pressure. Therefore, even when the amount of gas injected was the same, at different temperatures, the final pressures were not. Due to the temperature and pressure difference between the pump (5 ºC, 250 bar) and the view cell, the amount of limonene was calculated according to the number of moles of CO_2 injected at the pump temperature and pressure (ρ = 1020 mg/mL).[29] The amount of limonene added in the view cell was 2 mL (1.68 g, 0,012 mols), which was below saturation for all experiments.[2] The temperature and pressure of the pump is considered stable when the CO_2 flow rate is equal to zero. Table 3 shows the selected parameters for the experiment. The experiments were executed by acquiring the Raman spectrum at certain time intervals until the monitored peak for the compound presented stable intensity. The Raman spectrum was acquired in a set of 15 replicates for each measurement.

Extra experiments were performed in order to verify the repeatability of the measurements and also the effect of the stirrer. For the experiments with the stirrer on, a speed of 450 rpm was applied.

Table 2. Conditions of temperature, pressure and CO_2 volume for kinetic experiments with limonene.

Temperature (ºC)*	Pressure (bar)*	CO_2 (mL)
45	84	35
	94	55
	102	65
	125	75
55	95	35
	113	55
	130	65
	163	75

*Approximate values.

Table 3. Parameters for isothermal kinetic experiment with limonene

Laser		Detector					
Wavelength	Center	Grating	Binning	Slit	Acquisition time	Center	Cooler T
532 nm	3.5 W	1800 lines/mm	4	100 µm	1 s	597 nm	-75 ºC

3.4 Data acquisition and processing

The first step for data acquisition is to establish the instrument parameters, which are the laser power, grating, binning, acquisition time, slit, number of replicates and spectrum central wavelength.

The software chosen to process the data was OriginPro 2016. The dataset acquired was first exported from .sif to .asc format, which is recognized by the software. The wavelength (nm) values (X axis) were converted to wavenumber (cm^{-1}) eventually, according to Equation 1. The intensity values (Y axis), obtained in replicates, were baseline corrected and normalized. The chosen baseline correction was the Asymmetric Least Squares (ALS) smoothing method, which is basically an algorithm that estimates a smooth baseline for the spectrum with no prior knowledge of the data needed.[30] The normalization was done according to a reference signal present in the spectrum that does not belong to the compound. It can come from the sapphire or the CO_2, depending on the region the peak is situated. For each set of replicates, the average and standard deviation of the peak height was calculated. In order to remove possible outliers, the Grubb's test for single outliers was applied. The test compares the difference between the suspected value and the mean of replicates divided by its standard deviation (Equation 2).[31,32] The values for the statistic G were based in a 5% significance level.[32] The fit of the curve for the processed data was done by MATLAB R2016a, with the aid of the Curve Fitting Tool.

$$[cm^{-1}] = \left(\frac{1}{532\ nm} - \frac{1}{[nm]}\right) x\ 10^7 \qquad \textbf{Equation 1}$$

$$G = \frac{|suspected\ value - mean\ value|}{standard\ deviation} \qquad \textbf{Equation 2}$$

4 Results and Discussion

4.1 Sapphire fluorescence tests

Ideally, the sapphire window should not fluoresce but it does depending on the amount of impurities present in the crystal. In order to avoid this source of error, previous fluorescence tests were done in five selected windows from the same batch. Figure 7 shows Raman spectra of five sapphire windows in which fluorescence can be observed as high baselines.

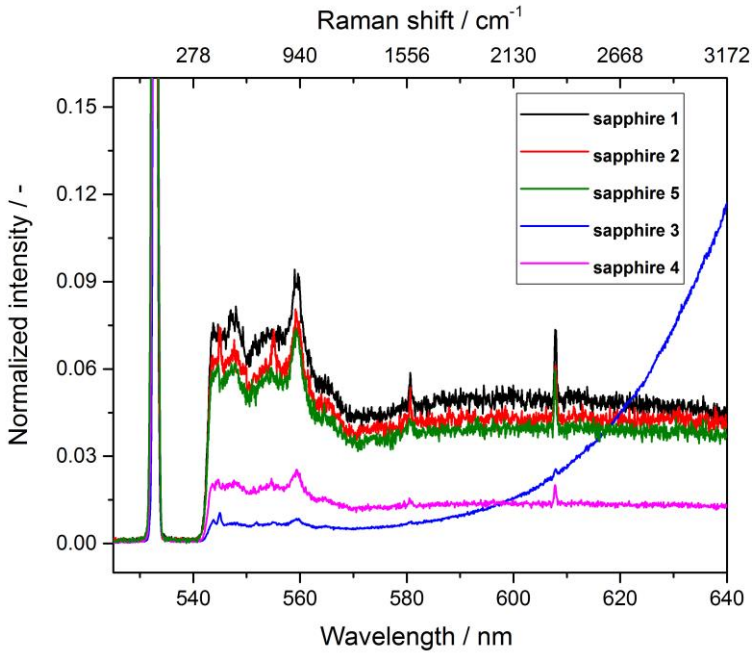

Figure 7. Raman spectra of sapphire windows.

Sapphires 3 and 4 presented the highest and lowest fluorescence respectively, while sapphires 1, 2 and 5 present similar intermediate fluorescence. Despite of not being too intense, this fluorescence may interfere in the compound peak to be properly compared with the solvent peak in a dissolution experiment where usually it is not very pronounced as well. During the experiments, windows with as low fluorescence as possible were picked.

4.2 Dissolution kinetics of limonene in $scCO_2$

4.2.1 Selecting a peak from limonene

First, the Raman spectrum of the pure limonene was acquired (Figure A 1. in the Appendix) and the peak chosen to be studied was a double peak situated between 583 and 584 nm. The two peaks correspond to C=C stretching modes, one from the cyclohexene ring and other from the ethylene group. [33-35] Figure 8 exemplifies the Raman spectrum of limonene in $scCO_2$ acquired in the experiments. The signal around 607 nm is a combination of a sharp sapphire peak and a smaller broad CO_2 peak. Thus, this peak was chosen to be the reference signal and all spectra were normalized according to it. Figure 8a shows the raw spectrum of limonene in $scCO_2$, while Figure 8b shows the same spectrum after correcting the baseline using the ALS method and normalizing.

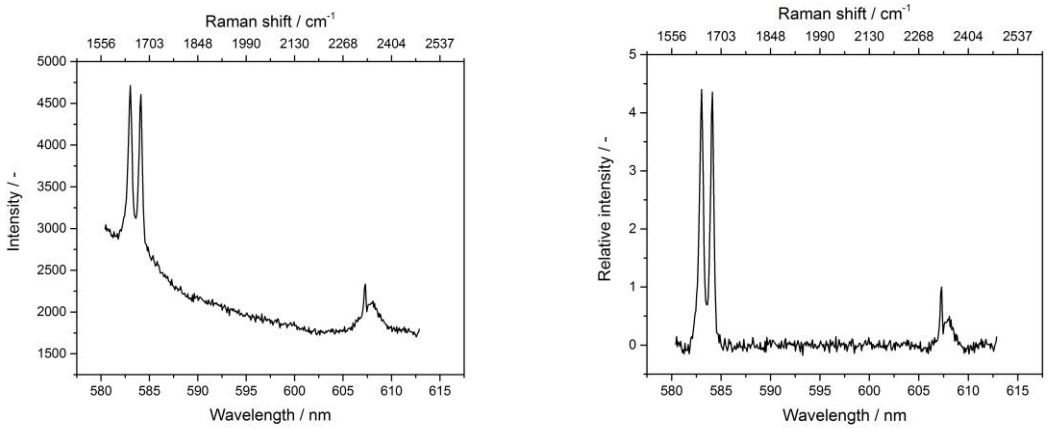

Figure 8. Raman spectrum of limonene in $scCO_2$ (a) before and (b) after processing the data – baseline correction and normalization.

4.2.2 Dissolution kinetic curves

In order to study the dissolution kinetics of limonene, the working hypothesis was expected to be the compound signal increasing with time until it reaches a plateau, which means that the conditions of dissolution equilibrium were achieved. The first experiments were done in a different setup consisting in a high-pressure variable-volume view cell (Figure A.2 in the Appendix). The view cell presented a horizontal design in relation to the sapphire window. The results were not consistent with the working hypothesis, where the limonene signal seemed not to go through notable changes with time, making any conclusion doubtful. A possible explanation was that the detector was not only acquiring signals from the sample present at the focal point, but also from sample in contact with the expanded beam. The implication is that both sample dissolved and not dissolved in CO_2 was being detected, which could explain the inconsistent results obtained with this view cell. This preliminary results led to the substitution of the high-pressure variable-volume

view cell for other with a different design (Figure 6). In this new design, the non-dissolved compound would seat at the bottom of the vessel, away from the pathway of the laser beam and therefore not be detected. Only signals coming from dissolved sample will be detected, as only a higher region of the view cell is exposed to the laser beam.

Then, the latter view cell design was used in all following experiments. The experiments were done in two temperatures and four amounts of CO_2 for each temperature, which led to different pressures, according to Table 2. The kinetic curves obtained after processing the data for the experiments at 45 and 55ºC are presented in Figures 9 and 10, respectively.

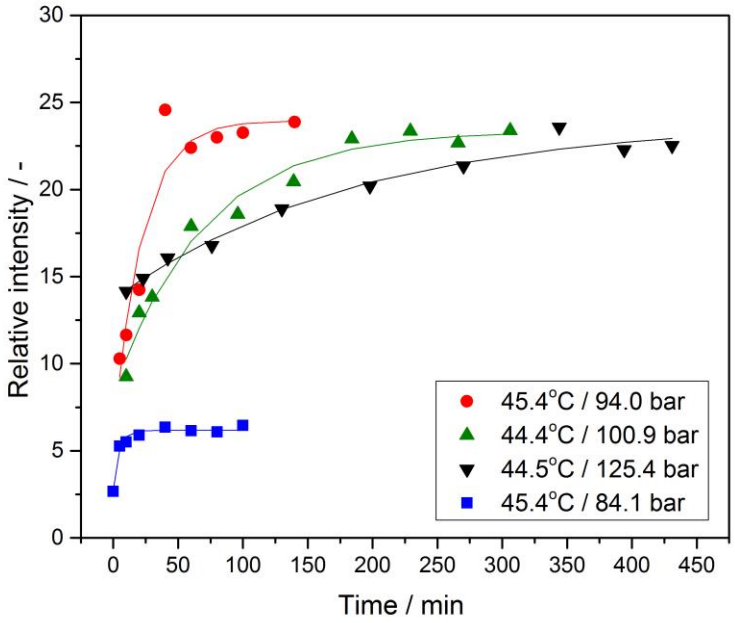

Figure 9. Dissolution kinetics curve for limonene at the approximate T = 45 ºC and 84.1 bar (■), 94.0 bar (●), 100.9 bar (▲), 125.4 bar (▼). Each data point is an average value of 15 replicates. The lines represent the fitted curves.

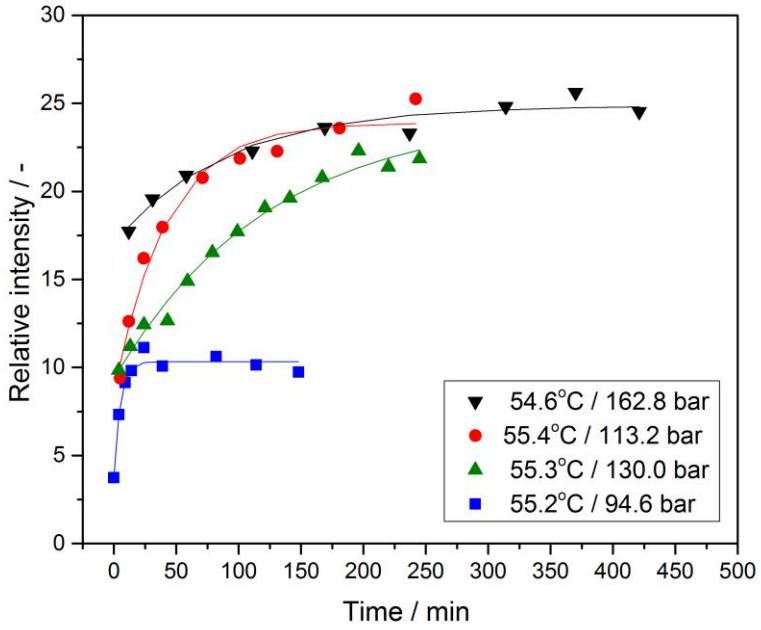

Figure 10. Dissolution kinetics curve for limonene at the approximate T = 55 ºC and 94.6 bar (■), 113.2 bar (●), 130.0 bar (▲), 162.8 bar (▼). Each data point is an average value of 15 replicates. The lines represent the fitted curves.

The study of dissolution kinetics of limonene in $scCO_2$ was feasible because the amount of compound dissolved is directly proportional to the peak intensity in the Raman spectrum. Such observation defines the developed methodology as a relative quantitative technique within an experiment, but without absolute number for concentration. Hence, the increase of peak intensity with time was observed in all experiments. Previous study in the literature has confirmed that Raman can work as a quantitative technique.[36] For that, a calibration curve is required. However, constructing a calibration curve with the present system, where the view cell is not at a fixed position, is not viable. The slight change in the view cell position between measurements would make the quantification not robust against variations in the operation conditions.

For each set of experiments at the same temperature it was noticed at first glance that the equilibrium plateau was reached faster with decrease in pressure. In terms of visual equilibrium time, for experiment 1 to 4, at 45 ºC, the plateau was reached around 25, 40, 180 and 340 minutes, respectively. For the experiment 5 to 8, at 55 ºC, the plateau was reached around 20, 60, 120 and 170 minutes, respectively. In order to confirm the observation and also compare the results between temperatures is necessary further study of the data by applying a curve fitting model, which is presented and discussed in the next session.

4.2.3 Curve fitting

A fitting procedure was carried out in all data in order to obtain a dissolution rate of the kinetic of solubility and to enable comparisons between the experiments at the same temperature and between temperatures. Exponential fitting of first and second order were applied. The first order exponential model was able to represent well all the curves, described by Equation 3, where the peak height (H) is presented as a function of time (t). Table 4 shows the coefficients values (A, B and C) and the dissolution rate (K) obtained, where K is 1/C. Comparing the set of experiments at the same temperature (Exp. 1 to 4 and 5 to 8), it is noticed an overall increase in the dissolution rate with decrease in pressure. Comparing experiment 7 and 8, the expected tendency is not noticed, where the highest pressure is slightly faster.

Increase of pressure corresponds to higher densities and therefore to higher values on saturation concentration.[2] However, the results contradict conventional theories of dissolution in regular liquids, in which concentration gradient is the driving force for dissolution, which suggests that there may be others mechanisms involved in dissolution kinetics of solutes in supercritical fluids. So far, no theory about it can be found in literature.

In terms of implication for an industrial process, by comparing the set of experiment at the same temperature, the lowest pressure reaches the plateau faster but with the lowest equilibrium solubility than the other pressures. This maybe not be the most advantageous option depending on the industrial application. Sometimes a higher solubility may be wanted over the use of mild conditions such as pressure and temperature, even if it requires more time and energy. For this reason, all parameters have to be taken into account before choosing the best conditions for a process.

$$H\,(t) = \; A - B * e^{t/C} \qquad \textbf{Equation 3}$$

Table 4. Values of coefficients A, B and C and dissolution rate (K).

Experiment	CO_2 (mL)	T (Celsius)	P (bar)	A	B	C	K (=1/C)	Stirrer
1	35	45.4	84.1	6.178	3.461	-4.486	-0.223	ON
2	55	45.4	94.0	23.96	18.6	-21.49	-0.046	
3	65	45.4	100.9	23.37	15.17	-68.72	-0.014	
4	75	44.5	125.4	23.92	10.24	-184.9	-0.0054	
5	35	55.2	94.6	10.33	6.603	-5.086	-0.197	ON
6	55	55.4	113.2	23.90	15.48	-41.62	-0.024	
7	65	55.3	130.0	24.40	15.05	-122.7	-0.0081	
8	75	54.6	162.8	24.86	7.859	-88.45	-0.011	
9	35	45.0	84.0	4.081	2.275	-135.2	-0.0074	OFF
10	35	55.0	95.2	8.309	4.936	-74.44	-0.013	
11	55	55.3	113.3	26.63	19.10	-67.90	-0.015	
12	55	45.1	93.6	13.65	18.92	-7.992	-0.125	ON
13	65	45.1	102.9	25.26	14.52	-104.2	-0.0096	
14	55	54.9	112.7	26.96	17.18	-53.35	-0.019	
15	55	55.2	113.5	28.11	18.11	-40.46	-0.025	

4.2.3.1 EXPERIMENTAL REPEATABILITY

In order to verify the precision of the measurements, some experiments were repeated at the exact same conditions as possible. Figures A3, A4 and A5 in the Appendix presents the results of repeated experiments 6/14/15, 3/13 and 2/12 shown on Table 4, respectively. The set of experiments 6/14/15 and 3/13 showed good proximity both for the curves and for the dissolution rate values. Repetitions 2 and 12 showed similar curves but different dissolution rates. While the relation between kinetic aspects and solubility at equilibrium is not known, the different dissolution rates may have to do with the fact that the average pressure at that temperature seems to be situated in a region of total miscibility, as seen in Figure 11 below, which is different from the solubility behavior observed at the pressure and temperature at which experiments 6/14/15 and 3/13 were performed.

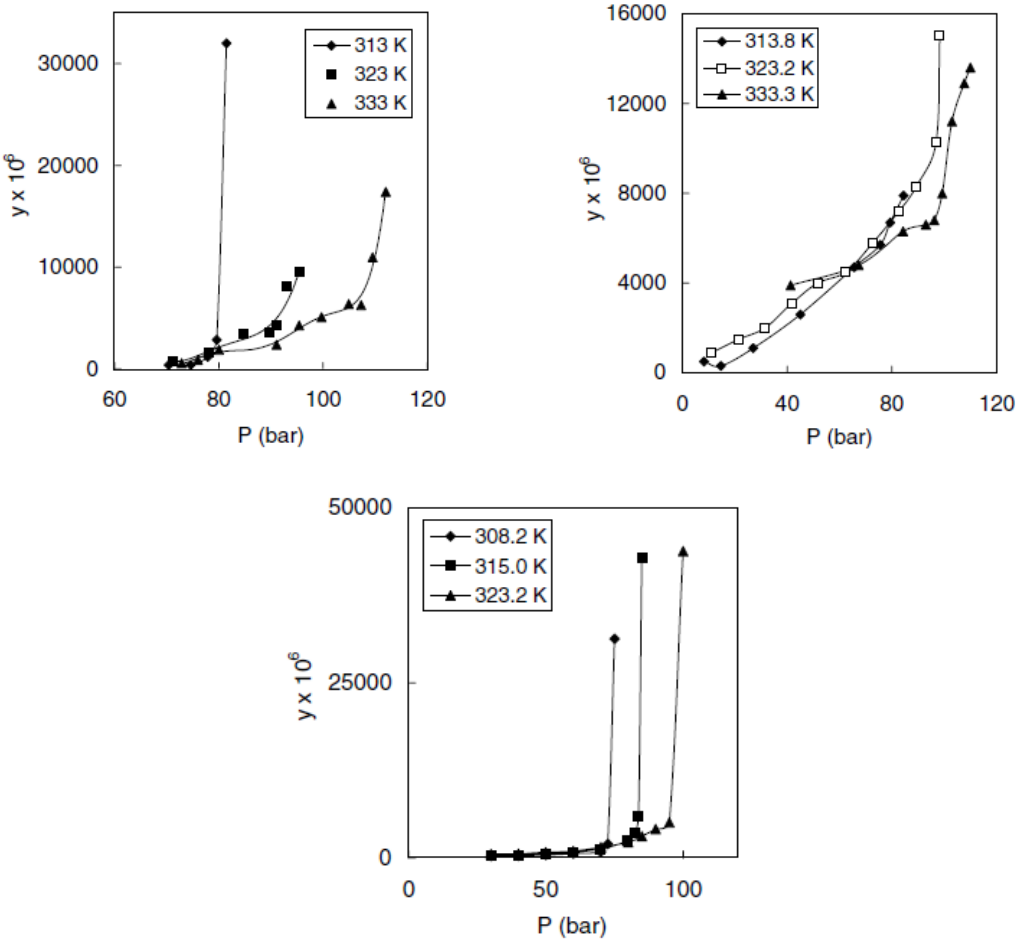

Figure 11. Solubility of limonene in $scCO_2$ in molar fraction (y) *vs.* pressure (P). [2]

4.2.3.2 STIRRER EFFECT

For crystals, the dissolution process of a particle in a liquid has the concentration gradient as the driving force and can depend on two different mass transport phenomena: diffusion and convection. Diffusion is a surface dependent process involving the crystal and detaching of ions or molecules. Convection is a transport dependent process responsible for exchange the particles from the diffusion layer adjacent of the crystal to the bulk.[7] Hence, the dissolution rate can be controlled by a surface or a transport process or a combination of both. The transport dependence can be noticed by stirring the solution.

For the mechanisms of dissolution of solids and liquids in supercritical fluids, on the other hand, there is a lack of theory in the literature. Due to the high diffusivity and low viscosity rates, one may believe that the dissolution process can be faster than conventional solvents for a given solute, but this is as far as can be estimated.

Thereby, the stirring effect was evaluated for three experiments based on the theory for crystals in a liquid. Figures A6, A7 and A8 in the Appendix presents the results of the experiments with stirrer on/off 6/11, 5/10 and 1/9 shown on Table 4, respectively. Experiments 6 and 11, at higher pressure, were not affected by the stirring with dissolution rates of same order of magnitude -0.024 and -0.015, respectively. This observation indicates that the dissolution process is limited by diffusion. If diffusion is slow, convection is hindered. For experiments 5 and 10 and 1 and 9, at lower pressures, dissolution rates had a great difference: -0.197 versus -0.013 and -0.223 versus -0.0074, respectively. This results shows that the process seems to be highly dependent on the convection, because diffusion must be faster.

However, determining the mechanisms of dissolution would require further studies, including developing theoretical models, which is out of the scope of this work.

4.2.4 Error bars

In the literature, a group of biologists have given great importance of how statistics as error bars, replicates and repetitions are represented in the scientific papers.[37-39] In one of their publications, they present some rules on how to use and interpret error bars.[37] One of them states that error bars may only be shown for experiments repeated independently and not for replicates. Replicates results from measures within a single experiment and because of that, do not infer any relevance of the hypothesis being tested. Instead, it only serves as an internal check on how the experiment was performed. Only independently repeated experiments are able to assess the reproducibility of the results.

Figure 12 exemplifies the error bars for each data point of the curve for the set of experiments 6,14 and 15. In this case, the error bars are the standard deviation (SD) of 15 measures (i.e. peak height) from 15 consecutive acquired Raman spectra. As the numbers obtained from the replicates are fluctuating and not constantly increasing, the idea that the errors could come from a steady increase in the dissolution of limonene in $scCO_2$ was discarded. Thus, one can say that SD

are solely related to internal fluctuations from the optical system of the setup, with no significance in the kinetics.

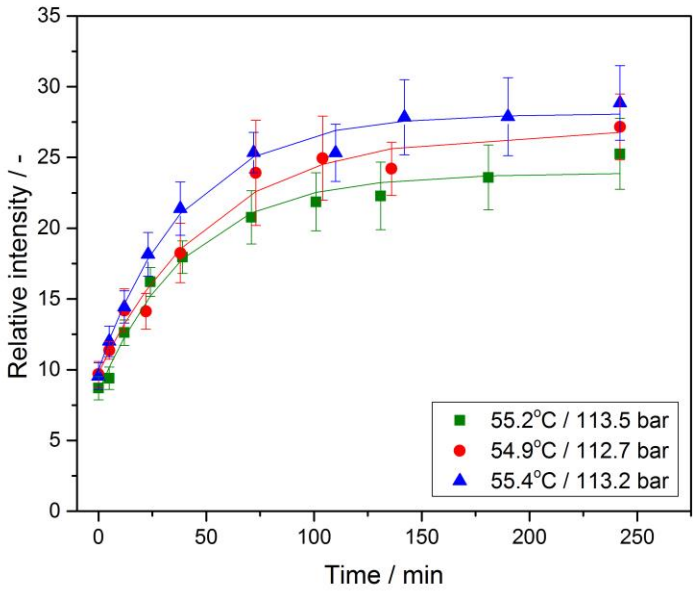

Figure 12. Error bars for the **r**epeated experiments at the approximate T = 55 ºC and 113.5 bar (▲), 112.7 bar (●) and 113.2 bar (■). Each data point is an average value of 15 replicates. The lines represent the fitted curves.

5 Conclusions

The developed methodology for the dissolution kinetic studies of limonene in $scCO_2$ using a high-pressure view cell by *in-situ* Raman spectroscopy proved to be effective. The design of the view-cell was relevant to enable the measurements.

The Raman spectroscopy with the CCD detector proved to be of great value by enabling the change of parameters, such as grating, binning and acquisition time, in order to improve the LOD.

The experiments were carried out at temperatures of 45 ºC and 55 ºC and pressure ranging from 84 to 163 bar. The time of the experiments ranged between 100 and 420 minutes. Curve fitting of the processed data showed that the solubility kinetics can be described by a first order exponential model. Dissolution rate values of the fitted curves showed that the kinetic of solubility becomes slower with increase of pressure and temperature. The results contradict conventional theories of dissolution in regular liquids, in which concentration gradient is the driving force for dissolution. So far, there is no theory that can describe the mechanisms involved in the dissolution of solids and liquids in supercritical fluids.

Repeated experiments showed good proximity both for the curves and for the dissolution rate values, except when the set temperature and pressure are situaded in the region of total miscibility in the graph of solubility *vs.* pressure.

Experiments to evaluate the stirrer effect on the dissolution showed that for lowest pressures at 45 and 55 ºC (84 and 95 bar respectively) the process is likely governed by convection and for higher pressures is likely diffusion controlled, based on the theory of crystals dissolution in liquids.

The methodology developed is considered relative quantitative within experiments, where the intensity of the limonene peak is directly proportional to the amount dissolved in the $scCO_2$.

6 Future aspects

As the new methodology developed showed suitable for dissolution kinetic studies, another soluble compounds in carbon dioxide can be tested. Test of solid compounds would provide new information regarding the diffusion and convection phenomena.

Another idea to verify the solubility kinetics with and without the presence of co-solvents such as ethanol. Addition of co-solvents increase the fluid polarity and therefore affects the solubility. Also to observe the dissolution behavior before and after the crossover point in order to see if there is a difference in the kinetic mechanism between these two regions. Before this point, an increase of temperature causes a decrease in solubility. After this point, the opposite effect occurs.

7 References

1. P. Styring, E. A. Quadrelli, K. Armstrong, Carbon Dioxide Utilisation: Closing the Carbon Cycle, Elsevier, Amsterdam, 1st edition, 2015, Chapter 1.

2. R. B. Gupta, J-J. m, Solubility in Supercritical Carbon Dioxide, CRC Press, New York, 2007, p. 1-5, 467-471.

3. P. Raveendran, Y. Ikushima, S. L. Wallen, Polar Attributes of Supercritical Carbon Dioxide, *Acc. Chem. Res.*, 38 (2005) 478-485.

4. M. Skerget, Z. Knez, M. Knez-Hrncic, Solubility of Solids in Sub- and Supercritical Fluids: a Review, *J. Chem. Eng. Data*, 56 (2011) 694-719.

5. G. Brunner, Applications of Supercritical Fluids, *Annu. Rev. Chem. Biomol. Eng.*, 1 (2010) 321-342.

6. Z. Knez, E. Markocic, M. Leitgeb, M Primozic, M. K. Hrncic, M. Skerget, Industrial applications of supercritical fluids: A review, *Energy*, 77 (2014) 235-243.

7. G.T. Hefter, R. P. T. Tompkins, The Experimental Determination of Solubilities, 2003, John Wiley & Sons, Chapter 1.2 and 5.1.

8. T. Fornari, R. P. Stateva, High Pressure Fluid Technology for Green Food Processing, Springer, Switzerland, 2015, p. 5-10.

9. P. Larkin, Infrared and Raman Spectroscopy: Principles and Spectral Interpretation, Elsevier, 2011, Chapter 1.

10. H. J. Butler, L. Ashton, B. Bird, G. Cinque, K. Curtis, J. Dorney, K. Esmonde-White, N. J. Fullwood, B. Gardner, P. L. Martin-Hirsch, M. J. Walsh, M. R. McAinsh, N. Stone, F. L. Martin, Using Raman spectroscopy to characterize biological materials, *Nature Protocols*, 11 (2016) 664-687.

11. IUPAC Compendium of Chemical Terminology (Gold Book), Version 2.3.3., 2014.

12. D. C. Harris, Quantitative Chemical Analysis, W.H. Freeman, New York, 8th edition, p. 103-104, 445-447. 454-459.

13. CCD Binning: what does binning mean? http://www.andor.com/learning-academy/ccd-binning-what-does-binning-mean. Accessed in 23 May 2016.

14. *What is a CCD detector?* Retrieved from http://www.horiba.com/de/scientific/products/raman-spectroscopy/raman-academy/raman-faqs/what-is-a-ccd-detector/ . Accessed in 23 May 2016.

15. R. D. Oparin, A. Idrissi, M. V. Fedorov, M. G. Kiselev, Dynamic and Static Characteristics of Drug Dissolution in Supercritical CO_2 by Infrared Spectroscopy: Measurements of Acetaminophen Solubility in a Wide Range of State Parameters, *J. Chem. Eng. Data*, 59 (2014) 3517-3523.

16. W. Liao, H.-W. Liu, H.-J. Chen, W.-Y. Chang, K.-H. Chiu, C. M. Wai, Catalytic hydrogenation rate of polycyclic aromatic hydrocarbons in supercritical carbon dioxide containing polymer-stabilized palladium nanoparticles, *Chemosphere*, 82 (2011) 573-580.

17. W. Liao, H.-B. Pan, H.-W. Liu, H.-J. Chen, C. M. Wai, Kinetic Study of Hydrodechlorination of Chlorobiphenyl with Polymer-Stabilized Palladium Nanoparticles in Supercritical Carbon Dioxide, *J. Phys. Chem. A*, 113 (2009) 9772-9778.

18. U. Schreiber, B. Hosemann, S. Beuermann, 1H,1H,2H,2H-Perfluorodecyl-Acrylate-Containing Block Copolymers from ARGET ATRP, *Macromol. Chem. Phys.*, 212 (2011) 168-179.

19. E. Moller, U. Schreiber, S. Beuermann, In Line Spectroscopic Investigation of Fluorinated Copolymer Synthesis in Supercritical Carbon Dioxide, *Macromol. Symp.*, 289 (2010) 52-63.

20. S. Beuermann, M. Buback, C. Isemer, A. Wahl, Homogeneous free-radical polymerization of styrene in supercritical CO_2, *Macromol. Rapid Commun.*, 20 (1999) 26-32.

21. S. Foltran, J. Alsarraf, F. Robert, Y. Landais, E. Cloutet, H. Cramail, T. Tassaing, On the chemical fixation of supercritical carbon dioxide with epoxides catalyzed by ionic salts: an in situ FTIR and Raman study, *Catal. Sci. Technol.*, 3 (2013) 1046-1055.

22. M. Caravati, J.-D. Grunwaldt, A. Baiker, Benzyl alcohol oxidation in supercritical carbon dioxide: spectroscopic insight into phase behavior and reaction mechanism, *Phys. Chem. Phys. Chem.*, 7 (2005) 278-285.

23. R. Sui, A. S. Rizkalla, P. A. Charpentier, Kinetics Study on the Sol-Gel Reactions in Supercritical CO_2 by Using In situ ATR-FTIR Spectrometry, *Cryst. Growth Des.*, 8 (2008) 3024-3031.

24. M. Champeau, J.-M. Thomassin, C. Jerome, T. Tassaing, In situ investigation of supercritical CO_2 assisted impregnation of drugs into a polymer by high pressure FTIR micro-spectroscopy, *Analyst.*, 140 (2015) 869-879.

25. M. Akgun, N. A. Akgun, S. Dincer, Phase behavior of essential oil components in supercritical carbon dioxide, *J. Supercritic. Fluids*, 15 (1999) 117-125.

26. C.-M. J. Chang, C.-C. Chen, High-pressure densities and P-T-x-y diagrams for carbon dioxide + linalool and carbon dioxide + limonene, *Fluid Phase Equilib.*, 163 (1999) 119-126.

27. A. Berna, A. Chafer, J. B. Monton, Solubilities of Essential Oils Components of Orange in Supercritical Carbon Dioxide, *J. Chem. Eng. Data*, 45 (2000) 724-727.

28. J. D. C. Francisco, B. Sivik, Solubility of three monoterpenes, their mixtures and eucalyptus leaf oils in dense carbon dioxide, *J. Supercrit. Fluids*, 23 (2002) 11-19.

29. *Peace software*. Retrieved from http://www.peacesoftware.de/einigewerte/luft_e.html. Accessed in 23 May 2016.

30. P. H. C. Eilers, H. F. M. Boelens, Baseline Correction with Asymmetric Least Squares Smoothing, Technical Report, 2005.

31. J. N. Miller, J. C. Miller, Statistics and Chemometrics for Analytical Chemistry, Pearson, England, 5th Edition, 2005, p. 51.

32. F. E. Grubbs, G. Beck, Extension of Sample Sizes and Percentage Points for Significance Tests of Outlying Observations, *Technometrics*, 14 (1972) 847-854.

33. H. Schulz, B. Schrader, R. Quilitzsch, B. Steuer, Quantitative Analysis of Various Citrus Oil by ATR/FT-IR and NIR-FT Raman Spectroscopy, *Appl.Spectrosc.*, 56 (2002) 117-124.

34. H. Schulz, M. Baranska, Identification and quantification of valuable plant substances by IR and Raman spectroscopy, *Vibrational Spectroscopy*, 43 (2007) 13-25.

35. P. V. Jentzsch, L. A. Ramos, V. Ciobota, Handheld Raman Spectroscopy for the Distinction of Essential Oils Used in the Cosmetics Industry, *Cosmetics*, 2 (2015) 162-176.

36. I. Rodriguez-Meizoso, J. Quino, A. Braeuer, In situ quantification of minor compounds in pressurized carbon dioxide using Raman spectroscopy, *J. of Supercritical Fluids*, 82 (2013) 263-267.

37. G. Cumming, F. Fidler, D. L. Vaux, Error bars in experimental biology, *The Journal of Cell Biology*, 177 (2007) 7-11.

38. D. L. Vaux, F. Fidler, G. Cumming, Replicates and repeats – what is the difference and is it significant? *European Molecular Biology Organization*, 13 (2012) 291-296.

39. D. L. Vaux, Know when your numbers are significant, *Nature*, 492 (2012) 180-181.

Appendix A. Figures

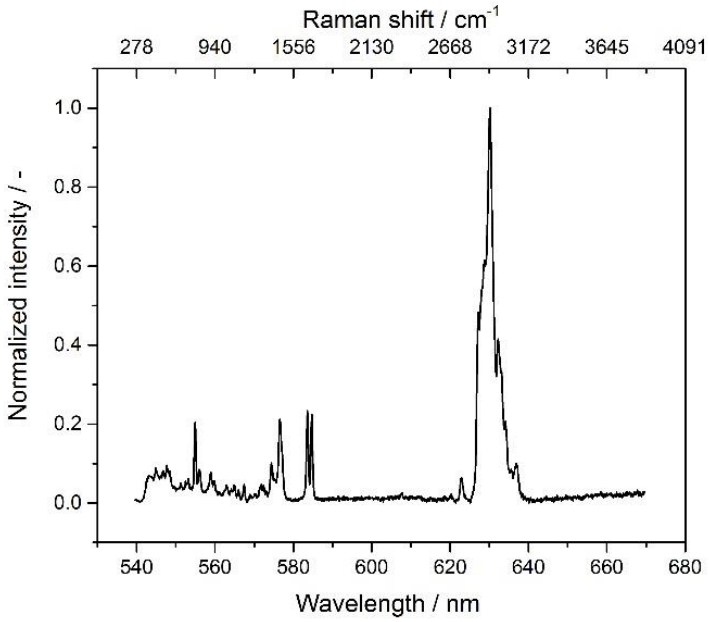

(a)

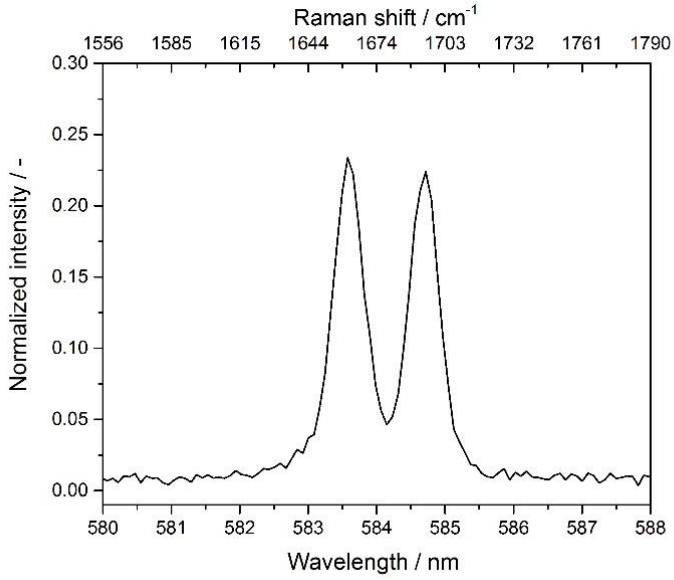

(b)

Figure A 1. Spectra of neat Limonene: (a) entire range and (b) zoom.

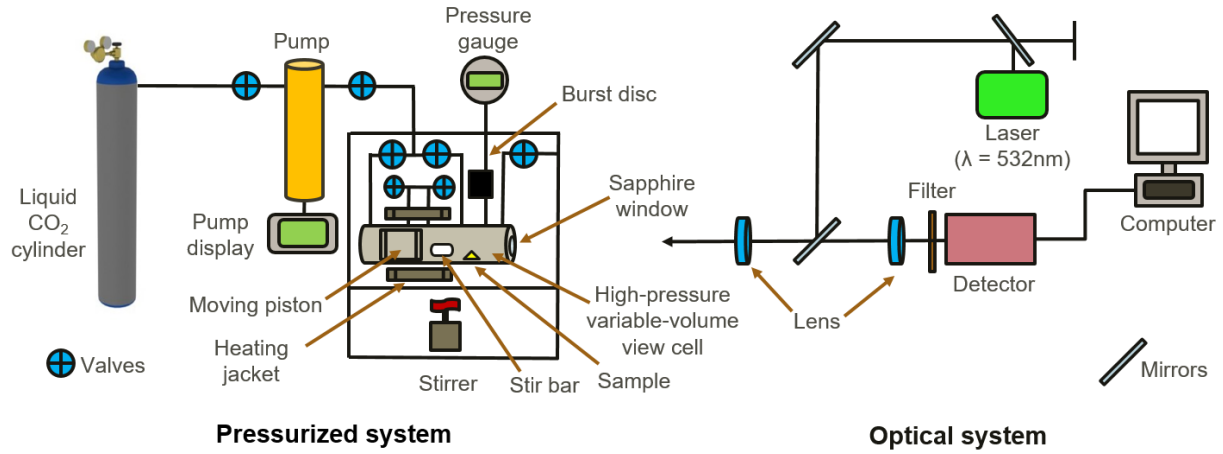

Figure A 2. Instrumental setup with a view cell of different design (high-pressure variable-volume view cell).

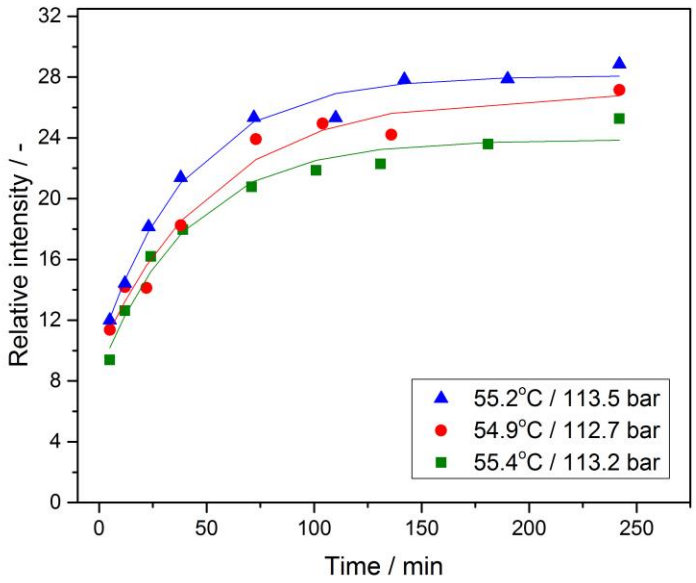

Figure A 3. Repeated experiments at the approximate T = 55 ºC and 113.5 bar (▲), 112.7 bar (●) and 113.2 bar (■). Each data point is an average value of 15 replicates. The lines represent the fitted curves.

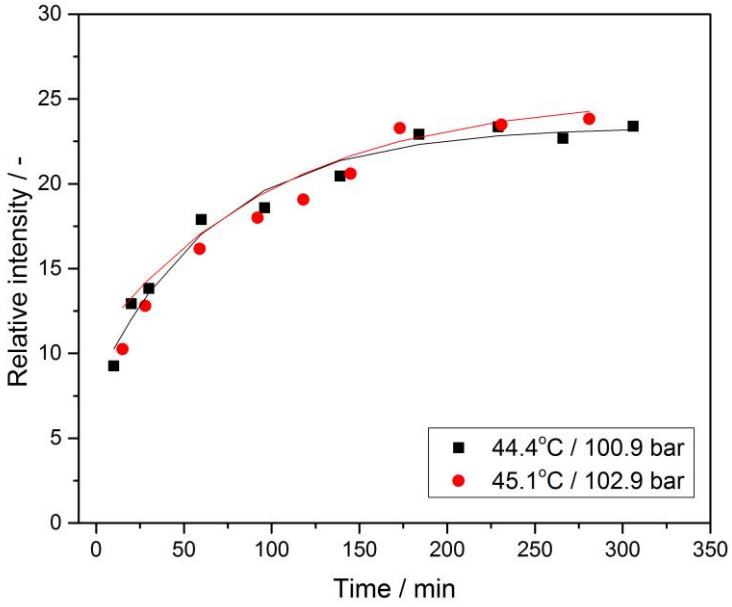

Figure A 4. Repeated experiments at the approximate T = 45 ºC and 100.9 bar (■) and 102.9 bar (●). Each data point is an average value of 15 replicates. The lines represent the fitted curves.

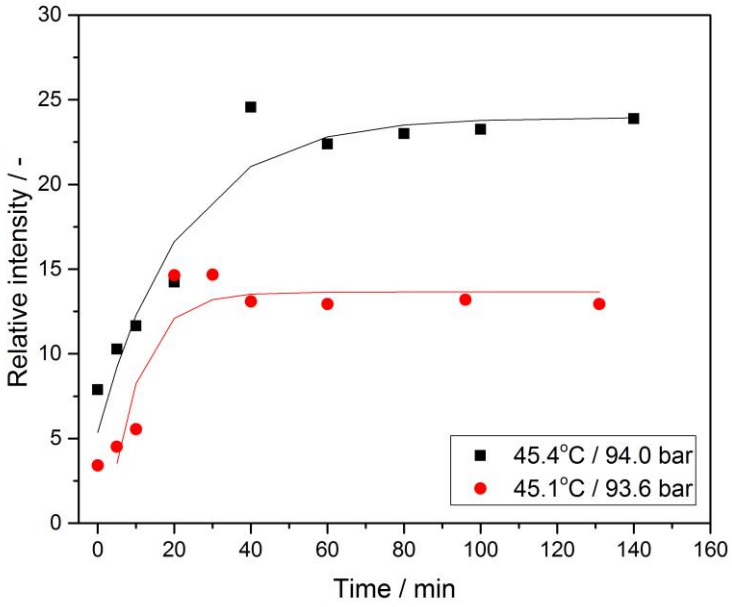

Figure A 5. Repeated experiments at the approximate T = 45 ºC and 94.0 bar (■) and 93.6 bar (●). Each data point is an average value of 15 replicates. The lines represent the fitted curves.

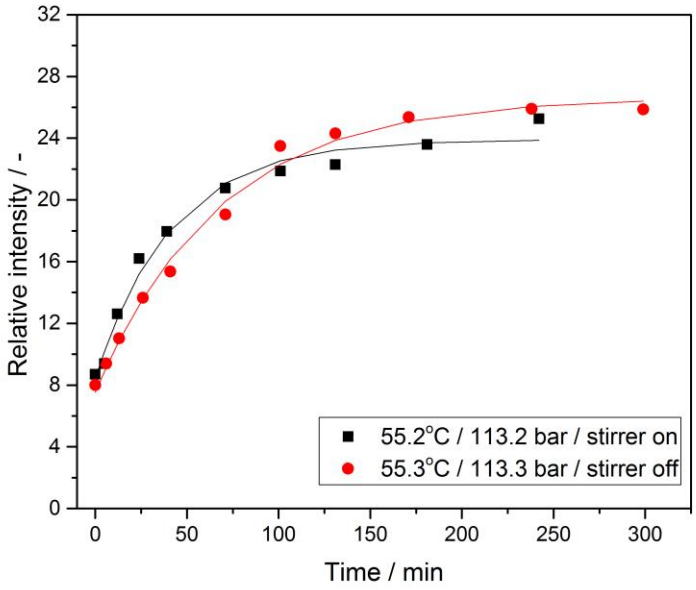

Figure A 6. Repeated experiments at the approximate T = 55 ºC and 113.2 bar and stirrer on (■) and 113.3 bar and stirrer off (●). Each data point is an average value of 15 replicates. The lines represent the fitted curves.

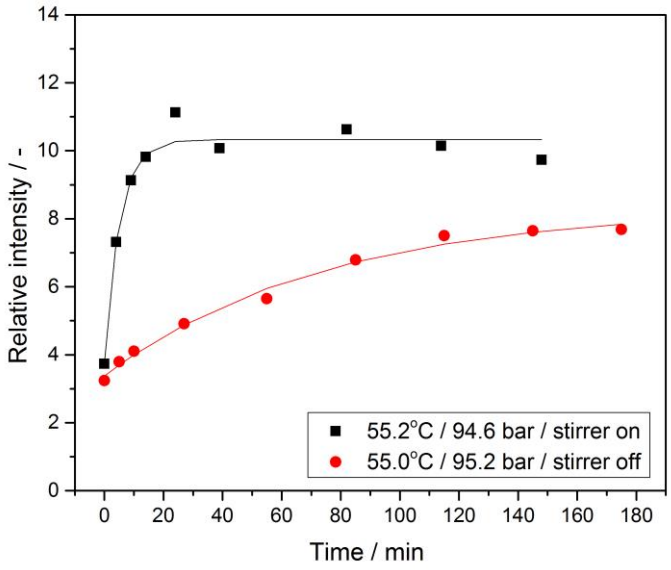

Figure A 7. Repeated experiments at the approximate T = 55 ºC and 94.6 bar and stirrer on (■) and 95.2 bar and stirrer off (●). Each data point is an average value of 15 replicates. The lines represent the fitted curves.

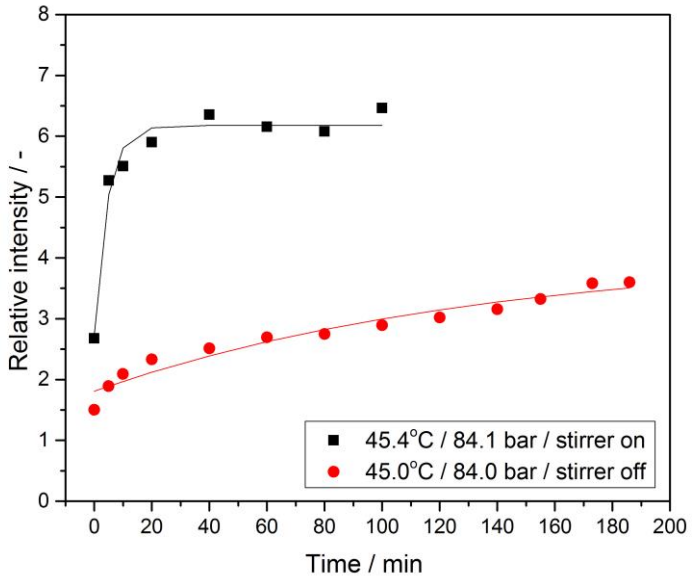

Figure A 8. Repeated experiments at the approximate T = 45 ºC and 84.1 bar and stirrer on (■) and 84.0 bar and stirrer off (●). Each data point is an average value of 15 replicates. The lines represent the fitted curves.

Appendix B Steps for using $scCO_2$ – Raman equipment

1. **Cleaning the vessel**

✓ Clean it with technical acetone/ethanol and paper. Let all parts dry in the fume hood

2. **Preparing the view cell**

✓ Add the sapphire and metal window with the rubber o-rings (clean it before with acetone). Clean the window with the appropriate tissue and acetone (no stains and/or tissue fibers must remain)

✓ Make sure that the windows are touching the bottom of the hole. Close with the lid very carefully and tight with the tool

✓ From the top, add the sample and the stir bar

✓ Close the lid on the top and tight with the tool

3. **Adjusting the vessel inside the equipment**

✓ Adjust the vessel inside, close all the openings properly first with the fingers and then tight with the tool

4. **Filling up the system with liquid CO_2**

✓ Open the cylinder valve and the valve placed on the left side of the tube to fill up (Refill button) with liquid. Recommended to fill up the cylinder a day before to let it cool appropriately

✓ Close the cylinder valve and the left valve of the tube

- ✓ Set up the pressure (A button – Enter value – Enter button)
- ✓ Open the right valve to pressurize the line connected to the vessel
- ✓ Let some CO_2 enter the vessel by opening the upper valve and check all valves/nuts/vessel for leakage
- ✓ Purge the system at least 3 times by adding some CO_2 to the vessel and releasing it by opening the lower valve on the left until the pressure is slightly above zero.
- ✓ Close all valves
- ✓ Place the heating tape around the vessel and tight it very well to avoid the risk of falling off during the experiment
- ✓ Place the thermocouple between the vessel and the heating tape, making sure it is touching both well
- ✓ Set up the temperature for the vessel and wait for it to stabilize. Remember that the temperature is set for the heating tape but the real temperature inside the vessel is measured by the thermocouple placed inside the vessel and displayed in the digital thermometer
- ✓ Start increasing the pressure inside the vessel and take a note of the initial CO_2 volume
- ✓ When the desired pressure/amount of CO_2 inside the vessel is reached, close the valve and take note of the final CO_2 volume
- ✓ Take note of the pressure after it stabilized

5. Turning on and aligning the laser

- ✓ Turn on the laser (2 buttons) and let it stabilize for some minutes ("enable" light stops blinking)
- ✓ Turn on the laser key from "standby" to "ready"
- ✓ Turn on the "emission" button
- ✓ To align the laser, set up a low power (120 mW) and change the filter position to the black side to block the laser
- ✓ Align the vessel/sample by moving it or changing the lens position
- ✓ After alignment, close the equipment with black plastic/paper and change the filter position to "transparent"

6. Taking a spectrum

- ✓ Turn on the camera and open the "Andor Solis" software in the computer
- ✓ Turn on the cooler and let its temperature stabilize
- ✓ Setup the laser power and the acquisition mode on the software (acquisition time, binning, grating…)
- ✓ Turn off all the lights (including the fume hood lights)
- ✓ Close the curtain
- ✓ Turn on the "laser on" light outside the room
- ✓ Turn on the laser (Button with red light)
- ✓ Take a picture/signal
- ✓ Turn off the laser
- ✓ Save your spectrum (.sif format)
- ✓ Export your spectrum in .asc format

7. Finishing the experiment

- ✓ Turn off: “emission” button, laser key, camera, chiller of the camera and vessel heating system
- ✓ Depressurize the vessel by opening the lower left valve. Connect a plastic tube to the nut to release the CO_2 inside the fume hood.
- ✓ Wait for the vessel to be warm enough to take it with your hands
- ✓ Remove everything connected to the vessel and open it
- ✓ Start from the beginning